Pipe Models for Entangled Fluids under Strong Shear

N. A. Spenley* and M. E. Cates

Department of Physics, Cavendish Laboratory, Madingley Road, Cambridge CB3 0HE, England

*Received February 10, 1994; Revised Manuscript Received April 6, 1994**

ABSTRACT: We study the rheology of polymers and other entangled fluids at high shear rate, where reptation theories (such as that of Doi and Edwards) predict, unphysically, a decreasing shear stress. A modification of the tube model, based on the concept of a dumbbell confined to a pipe, was recently proposed by Cates, McLeish, and Marrucci (*Europhys. Lett.* **1993**, *21*, 451). We show that their heuristic calculations correspond to a situation where the transverse dimension Δy of the dumbbell (perpendicular to the tube) remains constant in time. We perform an exact analysis, allowing Δy to fluctuate subject to the constraint of the pipe, and also study a more detailed model—a Rouse chain confined to a pipe. We find that the two dumbbell models give different results from each other and from the Rouse chain. We discuss briefly the relation between this work and experiments on entangled polymeric and micellar systems.

1. Introduction

The viscoelastic properties of entangled polymers are understood in terms of the reptation concept and, in particular, the theory of Doi and Edwards.[1] This theory is well-established for low and moderate strain rates, but at high strain rate, under shear flow, it has an anomalous feature: it predicts that the steady-state shear stress, σ_{xy}, falls with increasing strain rate, κ, as follows:

$$\sigma_{xy} \propto \kappa^{-1/2} \tag{1}$$

This is unphysical and indicates that an important effect has been left out.

The diagnosis is as follows: Doi–Edwards theory (without the independent alignment approximation[1]) includes the time evolution of tube segment orientations, as determined by two effects—first, the flow field, which causes a continuous deformation, and, second, the relaxation produced by reptation. The stress is calculated by assuming that the chain inside the tube is essentially unaffected by the flow and has a uniform tension along its length which maintains the contour length of the tube (or "primitive path") at its unperturbed value. At strain rates above the inverse Rouse time of the chain, this assumption can break down. For most flows, the deformation tends to increase the primitive path length, and at high deformation rates, the chain cannot relax quickly enough to maintain this at its equilibrium value. The Doi–Edwards theory, which assumes that this "first relaxation process" takes place infinitely fast, therefore breaks down in strong flows.

McLeish and Ball added a phenomenological stretching term in the Doi–Edwards constitutive equation to take account of this effect.[2] However, a more detailed analysis of primitive path stretching was done by Marrucci and Grizzuti[3] and by Pearson et al.,[4] who concluded that tube stretching is indeed important for flow with an elongational component but has negligible effect in steady shear flow. The reason is this: in shear flow, the tube tends to become fully oriented along the flow. The difference in flow velocity felt by the ends of the chain is therefore rather small, and the chain stretching effect is consequently weak. In the usual mathematics of the primitive path, the transverse dimension Δy of the path (in the shear gradient direction) actually tends to zero fast enough as $\kappa \to \infty$ that the primitive path remains completely unstretched in this limit. Thus the primitive path (or chain) dimension along the flow, Δx, approaches a constant value, as does the first normal stress difference, while the shear stress vanishes.

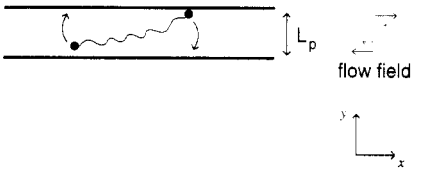

Figure 1. Pipe and dumbbell model proposed by Cates, McLeish, and Marrucci.

Despite these conclusions, it seems clear that strong enough shear flow must in practice produce significant deformations of the chain, resulting in increased stresses above those predicted from the stretching dynamics of the primitive path. In the next section we examine a recent simplified model intended to describe this, that of a dumbbell in a pipe. In section 3 we consider a more detailed model involving a constrained Rouse chain. Section 4 discusses and compares the models in the context of recent experiments. Section 5 gives our conclusions and suggestions for future work.

2. Dumbbell and Pipe Model

2.1. Heuristic Formulation. Cates, McLeish, and Marrucci (CMM) have argued that, since the tube becomes aligned with the flow at high shear rates, it can be modeled by a straight rigid pipe (Figure 1).[5] Although the transverse dimension of the primitive path (which is the axis of the tube) decreases indefinitely at high shear rates, the transverse dimension of the chain itself saturates at a value L_p on the order of the equilibrium tube diameter a. Thus there is still a stretching effect on the chain, because different parts of it are exposed to different flow velocities. This can be modeled by a chain confined to a pipe of width a, within which the velocity gradient deforms the chain by advection.

For simplicity, CMM model the chain inside the pipe as a dumbbell (of end-to-end vector $\Delta\mathbf{R}$), i.e., two beads on which viscous forces act, connected by a Hookean spring. They then argued that the transverse dimension of the dumbbell, Δy ($=L_p$) determined its dimension along the flow, Δx, according to

$$\Delta x \simeq \kappa \Delta y \tau \tag{2}$$

with τ the relaxation time of the dumbbell. This formula

* Abstract published in *Advance ACS Abstracts,* May 15, 1994.

0024-9297/94/2227-3850$04.50/0

reflects the relative displacement of the two beads, on streamlines separated by a displacement Δy, during the relaxation time τ.

If the root-mean-square end-to-end length of the chain is L_0, then the dumbbell has a spring constant of $3k_BT/L_0^2$. Moreover, the stress tensor σ is given by:

$$\sigma = \frac{3\nu k_B T}{L_0^2}\langle \Delta \mathbf{R} \Delta \mathbf{R} \rangle \tag{3}$$

where ν is the concentration of dumbbells. Therefore, the shear stress is

$$\sigma_{xy} = \frac{3\nu k_B T}{L_0^2}\Delta x \Delta y \tag{4}$$

$$\sigma_{xy} \cong 3\nu k_B T \kappa \tau (L_p/L_0)^2 \tag{5}$$

and the first normal stress difference $\mathcal{N}_1 = \sigma_{xx} - \sigma_{yy}$ obeys

$$\mathcal{N}_1 = \frac{3\nu k_B T}{L_0^2}(\Delta x \Delta x - \Delta y \Delta y) \tag{6}$$

$$\mathcal{N}_1 \cong 3\nu k_B T (\kappa\tau)^2 (L_p/L_0)^2 \tag{7}$$

where a small term independent of κ—which becomes negligible at high shear rate—has been dropped. (We will not consider the second normal stress difference in this paper. This is sensitive to whether motion in the z-direction should be constrained—in other words, whether the "pipe" is really a pipe or a pair of parallel plates. This question is discussed by CMM.)

Notice that, to within a numerical prefactor, these results are the same as those of the ordinary Rouse model, except that σ_{xy} and $\mathcal{N}_1$ are each reduced by a factor of $(L_p/L_0)^2$. Thus the effect of entanglement is to *decrease* both the shear and normal stresses from the values that would arise in the unentangled (Rouse) case. Combining these predictions with the Doi–Edwards theory at lower shear, CMM developed a scenario for the macroscopic flow behavior involving a shear banding instability.[5]

2.2. Rigorous Treatment. The above argument can be made rigorous (using a Langevin analysis along the lines outlined below) for the case where the transverse dimension of the dumbbell $\Delta y = L_p$ is constant in time. Thus, it is the correct analysis for a dumbbell whose beads are constrained to remain on streamlines separated by L_p for times up to the relaxation time τ. This model can be motivated if one thinks of each bead as being strongly coupled by entanglement to material on its own streamline.

Nonetheless, the original presentation of the model by CMM was in terms of a dumbbell confined to a pipe; in this model, therefore Δy is not a prescribed constant but is allowed to fluctuate, subject to the requirement that both beads must remain inside the pipe (of width L_p). We now outline an exact treatment of the pipe problem and show that it leads to rather different predictions from those of CMM. Whether these predictions are actually "better" than those of CMM is hard to decide; neither model is very close to a physical description of real chains. The fact that they differ is itself a strong indication that a more detailed description is needed.

Our dumbbell must obey the following Langevin equations, subject to the constraint of the pipe:[6]

$$\zeta \dot{\mathbf{R}}_1 - \frac{3k_B T}{L_0^2}(\mathbf{R}_2 - \mathbf{R}_1) = \mathbf{f}_1 + \zeta \kappa y_1 \hat{\mathbf{x}} \tag{8}$$

$$\zeta \dot{\mathbf{R}}_2 - \frac{3k_B T}{L_0^2}(\mathbf{R}_1 - \mathbf{R}_2) = \mathbf{f}_2 + \zeta \kappa y_2 \hat{\mathbf{x}} \tag{9}$$

where $\mathbf{R}_1 = (x_1, y_1, z_1)$ and $\mathbf{R}_2 = (x_2, y_2, z_2)$ are the bead coordinates, ζ is the friction coefficient of a bead, κ is the shear rate, and $\mathbf{f}_1$ and $\mathbf{f}_2$ are Brownian forces. If we let $\Delta\mathbf{R} = \mathbf{R}_2 - \mathbf{R}_1$, then:

$$\Delta \dot{\mathbf{R}} + \Delta \mathbf{R}/\tau = \mathbf{f}/\zeta + \kappa \Delta y \hat{\mathbf{x}} \tag{10}$$

where $\mathbf{f} = \mathbf{f}_2 - \mathbf{f}_1$, and $\tau = \zeta L_0^2/6k_BT$ is the relaxation time.

The dynamics of this system can be solved rigorously for large values of L_0/L_p. The details are given in Appendix A, but the essence of the method is as follows. The constraint—the pipe—couples only to motion of the beads in the y-direction. Motion in the x-direction is unconstrained. This means that we can simply integrate the x-component of eq 10 to obtain an expression, in the form of an integral, for $\Delta x(t)$ in terms of $\Delta y(t)$ and $\mathbf{f}(t)$. Then we can write down expressions for $\langle \Delta x \Delta y \rangle$ and $\langle \Delta x \Delta x \rangle$ in terms of $\langle \Delta y(0)\ \Delta y(t) \rangle$.

Since the flow is in the x-direction (and the interbead elastic force is linear), the behavior of the beads in the y-direction is independent of the shear rate. The tube width is much less than the radius of gyration of the chain, so we are interested in the limit $L_p/L_0 \to 0$. This makes the y-component of the elastic force negligible compared to the Brownian force, so the beads move independently in the y-direction. The problem of calculating $\langle \Delta y(0) \Delta y(t) \rangle$ is thereby reduced to that of a single particle undergoing Brownian motion in a one-dimensional box. This can be solved using Green's function of the diffusion equation. The final result is

$$\sigma_{xy} \cong \nu k_B T \kappa \tau (L_p/L_0)^{\alpha} \tag{11}$$

$$\mathcal{N}_1 = n_1 \nu k_B T + n_2 \nu k_B T (\kappa\tau)^2 (L_p/L_0)^{\beta} \tag{12}$$

where

$$\alpha = 4 \tag{13}$$

$$\beta = 4 \tag{14}$$

and n_1 and n_2 are numerical constants whose values can be calculated. This is the rigorous (asymptotic) solution of the dumbbell and pipe model, for a pipe much narrower than the radius of gyration of the chain.

We have defined exponents α and β to describe the dependence of the shear and normal stresses, respectively, on L_0/L_p. Here we have $\alpha = \beta = 4$, which is twice the value derived by CMM. Their analysis cannot be applied to this model, because it rests on a static picture of the dumbbell, when the behavior is in fact dominated by fluctuations. Specifically, when the pipe is narrow, Brownian forces cause the dumbbell to "wobble" or rotate within the pipe (see Figure 1) on a short time scale (on the order of $\tau(L_p/L_0)^2$), causing the velocity difference between the two ends to be rapidly reversed. The dumbbell, therefore, never has time to stretch as much as it is supposed by CMM, and the stresses are therefore less (by a factor of $(L_p/L_0)^2$).

The discrepancy between the two dumbbell descriptions suggests that neither may offer a reliable picture of a chain in a tube (although without a tube, the dumbbell does correctly reproduce the stresses predicted from the Rouse model). The tube will tend to cut off fluctuations in the structure of the chain on scales longer than the tube diameter, so short-length-scale effects (ignored in the

dumbbell approach) might become important. In any case, the rapid wobble motion described above seems unrealistic in a model of flexible chains. A more accurate description—such as the Rouse chain in a pipe—is needed, and we address this model next.

3. Rouse Chain in a Pipe

3.1. Simulation Results. The method used in Appendix A for the dumbbell cannot be extended to the Rouse chain. In the absence of a confining pipe, the Rouse modes are independent, so the model can be solved exactly. With the pipe present, the modes are coupled by the constraint, and the model is no longer soluble analytically (although a related model *is* soluble and is studied in the next section). However, it can be studied by simulation. We present here the results of a Brownian dynamics study for the Rouse chain in a pipe.

It is shown in Appendix B that, if the pipe is aligned with the shear flow, the shear stress is proportional to the shear rate (i.e., the viscosity is constant), while the first normal stress difference is of the form:

$$\mathcal{N}_1 = C_1 + C_2\kappa^2 \tag{15}$$

where C_1 and C_2 do not depend on κ. Note that C_1 is an equilibrium property and as such can be calculated analytically. It arises because of the loss of free energy involved in confining the chain; the chain exerts a pressure on the sides of the pipe. For the Rouse chain in the continuous limit (i.e., an infinite number of beads and springs), it has the asymptotic value:[1]

$$C_1 = (\pi^2/3)\nu k_B T(L_0/L_p)^2 \tag{16}$$

when L_p, the pipe width, is much less than L_0, the root-mean-square end-to-end length of the chain.

Simulations have been done for a range of pipe widths. Our aim is to investigate the properties of the continuous limit of the Rouse chain, so, for each width, chains with various numbers of springs have been tried (including the case of a single spring, i.e., the dumbbell). In each case, however, the following units of time, length, and energy have been chosen: the relaxation time of the chain (i.e., its Rouse time τ_R), the root-mean-square end-to-end length, and k_BT. This choice ensures that, in the limit of a very large number of springs, the result will become independent of that number and will approach the appropriate continuum limit. The time step and the averaging time were chosen separately for each trial; for the 60-spring chain, they were $10^{-3}\tau_R$ and $500\tau_R$, respectively. For every case, a range of shear rates was used, from $0.1\tau_R^{-1}$ to $10^4\tau_R^{-1}$, and the appropriate forms for the shear stress and the first normal stress difference were fitted. The results are given in Figures 2 and 3. As we would expect, for $L_p \gg L_0$, the pipe has no effect on the chain, and the stress is independent of L_p. For $L_p < L_0$, there is a power law dependence. Clearly though, a multiple-spring chain behaves quite differently from a dumbbell. For the dumbbell, α and β are found to equal 4, as expected, while for the many-spring chain, $\alpha = 2$. $\mathcal{N}_1$ is apparently more sensitive to the number of springs (or to having a very narrow pipe); at any rate, the simulation result failed to converge with increasing spring number for the parameters we tried. Thus we did not extract a value of β from the simulations. Rather than attempt to resolve this with larger simulations, we turn instead to a slightly different model which can be solved analytically.

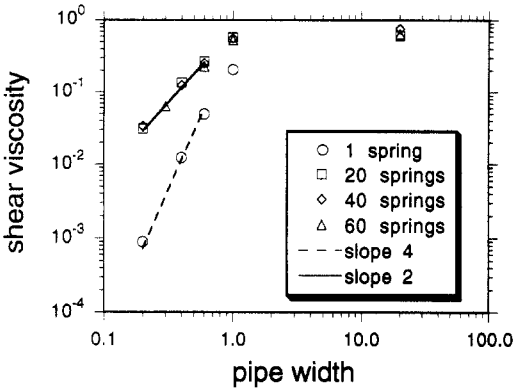

Figure 2. Results of simulations for the Rouse chain (with various numbers of springs and beads) in a pipe. Units are chosen so that the concentration of chains, the Rouse time, the root-mean-square end-to-end length (in the absence of the pipe and with no flow), and the thermal energy are all unity.

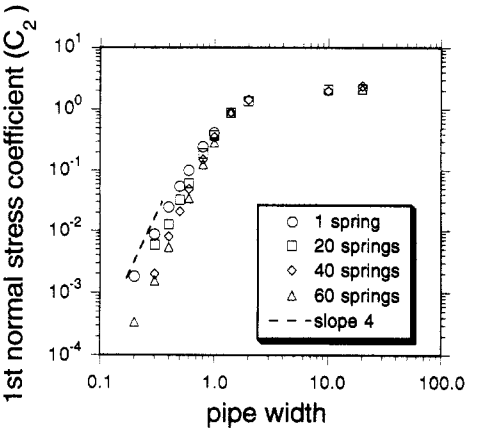

Figure 3. Same as in Figure 2. The coefficient plotted is C_2 of eq 15.

3.2. The Quadratic Pipe. The essential property of the pipe is that it confines the chain, exposing it to a narrower range of flow velocities. If we replace the pipe (with sharply-defined, hard walls) by a potential which has the same confining effect, we expect the result to be essentially unchanged. In fact, we will use a potential quadratic in y. This has the advantage that, because the force on any bead is now linear in its position, the Rouse modes are still independent, and this means that the model is soluble.

To check the validity of the quadratic potential, we first solve for the dumbbell. The Langevin equation is now

$$\Delta\dot{\mathbf{R}} + \Delta\mathbf{R}/\tau = \mathbf{f}/\zeta + \kappa\Delta y\hat{\mathbf{x}} - \lambda\Delta y\hat{\mathbf{y}} - \lambda\Delta z\hat{\mathbf{z}} \tag{17}$$

without any constraints, where λ is a parameter measuring the strength of the quadratic potential. Note that, because the confining force is linear in position, it can be considered as the viscous force on the beads caused by an effective flow field. The velocity gradient tensor for this effective flow is

$$\mathbf{K}^{\text{eff}} = \mathbf{K} + \mathbf{L} \tag{18}$$

where $\mathbf{K}$ is the physical flow and $\mathbf{L}$ represents the confining force:

$$\mathbf{K} = \begin{pmatrix} 0 & \kappa & 0 \\ 0 & 0 & 0 \\ 0 & 0 & 0 \end{pmatrix} \tag{19}$$

$$\mathbf{L} = \begin{pmatrix} 0 & 0 & 0 \\ 0 & -\lambda & 0 \\ 0 & 0 & -\lambda \end{pmatrix} \tag{20}$$

Since the dumbbell model can be solved for any flow (see, e.g., ref 6), the stress can be found easily. First, we must estimate the parameter λ, which we do as follows. $\langle \Delta y \Delta y \rangle$ is found to be $L_0^2/3(1 + 2\lambda\tau)$. But $\langle \Delta y \Delta y \rangle$ must be chosen to be on the order of L_p^2, since L_p is the required pipe width (we assume $L_p \ll L_0$). In this limit, $\lambda \gg 1$, giving us:

$$\lambda \cong \frac{1}{\tau}\left(\frac{L_0}{L_p}\right)^2 \tag{21}$$

The stress is found to be

$$\sigma_{xy} \cong \nu k_B T \kappa \tau (L_p/L_0)^4 \tag{22}$$

$$\mathcal{N}_1 = \nu k_B T + n_3 \nu k_B T (\kappa\tau)^2 (L_p/L_0)^4 \tag{23}$$

where n_3 is a numerical constant. Apart from numerical factors, this is identical to the result for the hard pipe (eqs 11 and 12).

We now proceed to the Rouse model. The Langevin equation for a Rouse chain is[1]

$$\zeta \frac{\partial \mathbf{R}_n}{\partial t} - k \frac{\partial^2 \mathbf{R}_n}{\partial n^2} - \zeta \mathbf{K}^{\text{eff}} \cdot \mathbf{R}_n = \mathbf{f}_n \tag{24}$$

where $\mathbf{R}_n$ is the position of the nth bead, and $\mathbf{f}_n$ is the Brownian force on the nth bead. We have included the force due to the quadratic confining potential; the strength of this potential, λ, will not be the same as in the dumbbell model but must again be chosen to give the correct dimension of the chain in the y-direction (velocity gradient direction). As with the dumbbell, the confining force acts on the beads in exactly the same way as an effective flow, so the equation can be solved in the usual way, by separating into normal modes. Summing up the modes to give the final result is nontrivial. It can be done in the limiting case of interest $\lambda \to \infty$ (i.e., $L_p/L_0 \to 0$), for which the sums can be replaced by integrals (the details are given in Appendix C).

The stresses are found to be

$$\sigma_{xy} \cong (c/N) k_B T \kappa \tau_R (L_p/L_0)^2 \tag{25}$$

$$\mathcal{N}_1 = n_4 (c/N) k_B T (L_p/L_0)^{-2} + n_5 (c/N) k_B T (\kappa\tau_R)^2 (L_p/L_0)^6 \tag{26}$$

where τ_R is the Rouse time of the chain, and n_4 and n_5 are numerical constants. The value of α is therefore 2, as discovered in the Rouse simulation, and unlike the dumbbell in a pipe (for which $\alpha = 4$). The normal stress exponent, β, is 6, compared to 4 for the dumbbell in a pipe. These changes in exponent mean that the first normal stress difference is smaller for the Rouse chain than for the dumbbell, in qualitative agreement with the simulation result (Figure 3).

Our results demonstrate that a dumbbell model is not sufficient if one wants to describe accurately the rheological behavior of a chain confined to a (quadratic) pipe under the convective influence of a steady shear flow. This behavior is in contrast to a free chain, for which Rouse and dumbbell predictions coincide.

3.3. Scaling Ideas. We now try to understand qualitatively the results of sections 3.1 and 3.2. A chain confined to a pipe can be loosely thought of as forming a series of blobs, each with diameter equal to the width of the pipe (Figure 4). In the absence of a flow, each blob can be considered independent of the others. This provides a scaling law—any equilibrium free energy (or stress) must be a property of the blobs only and thus (at fixed chain concentration ν) proportional to N, the degree of polymerization of the chain.[7]

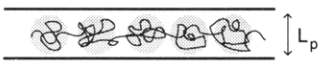

Figure 4. Blob concept, for a polymer in a tube.

For example, the anisotropy in pressure exerted by the chain at equilibrium (in other words, C_1 in eq 15) can be calculated as follows. It must be proportional to $\nu k_B T$, which has the dimensions of stress. Furthermore, there are two important lengths—L_0, the chain's root-mean-square end-to-end length, and L_p, the pipe width. Therefore, for $L_0 \ll L_p$, the first normal stress should take the scaling form:

$$\mathcal{N}_1 \cong \nu k_B T (L_0/L_p)^\gamma \tag{27}$$

where γ is some exponent. Now we use the scaling law. For an ideal chain, L_0 is proportional to $N^{1/2}$, so we deduce that γ must equal 2.[7] This is in agreement with the rigorously derived result for the quadratic pipe (eq 16).

Any equilibrium property can be similarly calculated, to within numerical prefactors. Inspired by this, we make the following conjecture concerning dynamic properties. We argue that the effect of the pipe on the chain is to cut off all of the chain's structure on length scales greater than the pipe diameter, even when a flow field is present. This means that any region of the chain behaves independently of other regions further away than the pipe diameter. Thus the chain is again composed of a number of independent sections ("blobs"), even though not at equilibrium. The stress must therefore still be proportional to N. We assume that it can be written in the following form:

$$\sigma_{xy} \cong \nu k_B T \kappa \tau_R (L_p/L_0)^\alpha \tag{28}$$

$$\mathcal{N}_1 \cong \nu k_B T (\kappa\tau_R)^2 (L_p/L_0)^\beta \tag{29}$$

where we have omitted the equilibrium (κ-independent) part of $\mathcal{N}_1$. These forms for the shear and normal stresses ensure that the usual Rouse result is recovered when $L_p/L_0 \cong 1$, that is, when the pipe becomes too wide to confine the chain. Now, given (from ref 1) that the Rouse time, τ_R, is proportional to N^2, we ask what values α and β must take so that both σ_{xy} and $\mathcal{N}_1$ are proportional to N. The answer is

$$\alpha = 2 \tag{30}$$

$$\beta = 6 \tag{31}$$

Thus, we have reproduced the main results of section 3.2.

It is interesting that the Rouse chain in a pipe gives the same result for the shear stress ($\alpha = 2$) as that of CMM, while $\mathcal{N}_1$ is found to be much smaller (by 4 powers of L_p/L_0). The difference between the Rouse chain and the dumbbell result with a true pipe constraint (for which $\alpha = \beta = 4$) can be interpreted as follows: the Rouse chain has many short-length-scale fluctuations in its structure, which are absent in the dumbbell. These fluctuations can carry extra stress, which increases the shear stress by a factor of $(L_0/L_p)^2$ relative to the dumbbell. On the other

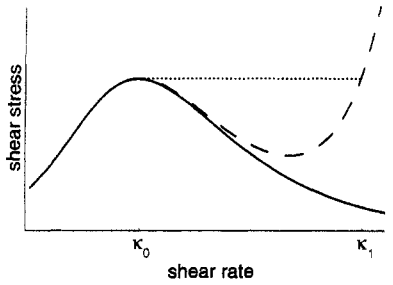

Figure 5. Shear stress predicted by the reptation-breaking theory for micelles (solid line), the expected turnup at high shear rate (dashed line), and the effect of shear banding (dotted line). The corresponding curves for unbreakable polymers are very similar.

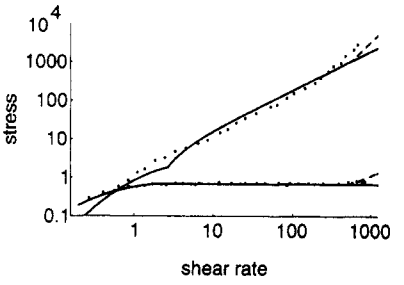

Figure 6. Experimental data of ref 14 (points) and the prediction of reptation breaking and shear banding (solid lines). The upper curve is the first normal stress difference, while the lower is the shear stress. The dashed curve is fitted on the assumption that the final data points are the start of the expected stress turnup. Units are the reciprocal terminal relaxation time τ_M^{-1} (for the strain rate) and the high-frequency plateau modulus (for the stress).

hand, the fluctuations tend to increase the volume occupied by the chain. This makes the confinement effect stronger, so—as far as the low modes are concerned—each mode is effectively confined to a pipe much narrower than the real width, tending to reduce the stress. This effect dominates the first normal stress difference, which is smaller than for the dumbbell, by a factor of $(L_0/L_p)^2$.

The very weak stretching of the confined Rouse chain can be associated with a wobble mode similar to that discussed earlier in comparing the CMM model with a dumbbell in a true pipe. Here the stretching effect is still further diminished since the chain within each blob can wobble independently, leading to a reduction in the mean convective displacement of parts of the chain on different streamlines.

4. Discussion: Experimental Comparisons

Doi–Edwards theory[1] predicts a shear stress that increases with strain rate up to a maximum and then falls away toward zero (similar to Figure 5, solid curve). The maximum occurs at a strain rate κ_0, on the order of the reciprocal reptation time. The local deformation effects discussed above will take over at some higher shear rate κ_1, so we expect the shear stress–strain rate curve to have the form of Figure 5, dashed curve. The decreasing region of the shear stress must be unstable, however,[8] so for an applied strain rate in the range κ_0 to κ_1, we expect the flow to be "shear-banded". This means that there are parts of the flow with strain rates κ_0 and other parts with κ_1, with volume fractions such that their *average* strain rate equals whatever rate is applied. We suppose that, in Couette or cone-and-plate flow, as the shear rate is increased from zero, the entire flow remains on the low-shear stable branch of the curve for as long as possible. When κ_0 is reached, a small amount of material must begin to shear at κ_1. As the shear rate is increased further, the proportion of κ_1 increases, until the whole of the sample is being sheared at this rate. The flow is now uniform again and remains so if the shear rate is increased still more. (See ref 5.) The hallmark of this behavior is that, in the shear-banded regime, the shear stress is independent of strain rate (and equals the maximum predicted by Doi and Edwards; Figure 5, dotted curve), while the first normal stress difference $\mathcal{N}_1$ is an average over the shear bands and is therefore roughly linear in the strain rate. (This assumes that $\mathcal{N}_1$ is much larger in the high shear branch than at low shear.)

Such behavior has not been widely reported for ordinary polymers, although very recent work of Bercea et al. gives an indication of something similar.[9] This may be because of experimental difficulties, which are discussed in ref 5. In the absence of quantitative data for ordinary polymers, we turn to a polymer-like system, namely, wormlike surfactant micelles (ref 10 is a review). These are highly elongated aggregates, which are rather similar to polymers, except that they can spontaneously break and reform. This ensures that the micellar weight distribution is in equilibrium (and has an exponential form). Wormlike micelles can entangle, in the same way as polymers; the terminal relaxation process is not pure reptation but reptation in conjunction with chain-breaking reactions. A reptation theory, based on Doi–Edwards theory, has been developed, which takes into account these reversible breaking reactions.[11] The predictions of this theory for the linear behavior have been carefully compared with experiment.[12,13] In the nonlinear regime, a stress–strain rate curve for steady shear flow is predicted that is very similar to that of Doi and Edwards. This is the curve shown in Figure 5. As with the polymers, the shear stress must turn up at high strain rate (through some effect neglected in the basic theory), so we expect micelles to show the shear-banding effect.[15]

Comprehensive nonlinear viscoelastic data are available for one particular system, based on cetylpyridinium chloride in aqueous solution with sodium salicylate.[14] The steady shear behavior has been compared with the theory[15] and agrees convincingly (Figure 6). It should be noted that, without a detailed model of the high shear rate behavior, we can still predict the value of κ_0, the exact shape of the shear stress and $\mathcal{N}_1$ below it, and the height of the shear stress plateau above it (plus, of course, the roughly linear form of $\mathcal{N}_1$, although not its slope). All of these were found to agree, with no fitting required (the two parameters needed—the relaxation time and the (high-frequency) plateau modulus—can be obtained from the linear viscoelastic data).

It was speculated[15] that, if micelles can be considered unbreakable on the time scale of the shear deformation—in other words, if $\kappa \gg 1/\tau_b$, where τ_b is the characteristic time required for a micelle to break—the chains will behave like ordinary polymers in the high shear regime. The results of CMM for the dumbbell in a pipe (eqs 5 and 7) were therefore used in ref 15 to estimate two further parameters. By fitting a straight line to $\mathcal{N}_1$ above κ_0 and taking its slope, it was deduced that:

$$\tau_R/\tau_M \approx 0.5 \tag{32}$$

where τ_R is the Rouse time and τ_M is the Maxwell relaxation time associated with the reptation-breaking theory. To extract any more information, it is necessary to estimate the value of κ_1—the end of the shear stress plateau and the onset of the subsequent turnup—from the data. Unfortunately, the experimental results of ref 14 are ambiguous; the final few data points may or may not be

part of the turnup. By assuming that they were, it was found that:

$$N_T = 25 \tag{33}$$

where N_T is the number of entanglements per chain. This agrees with a separate estimate based on linear viscoelastic data.[12]

These estimates were made using the predictions given by CMM for the high shear branch, $\alpha = \beta = 2$ corresponding to a dumbbell with fixed Δy. Following the work of previous sections, we have now two further candidate models for this regime: the dumbbell with a true pipe constraint ($\alpha = \beta = 4$) and the Rouse chain in a (quadratic) pipe ($\alpha = 2, \beta = 6$). Given the uncertainties over modeling the high shear behavior, we now attempt to reinterpret the data of ref 14, leaving for generality α and β as arbitrary parameters.

First, we must estimate κ_1. This is the strain rate at which the shear stress of eq 25 is equal to the shear-banding plateau, which is equal to the maximum stress predicted by the reptation theory (or, for micelles, the reptation-reaction model[15]). This maximum is on the order of the plateau modulus, ck_BT/N_e, where c is the monomer concentration and N_e is the entanglement degree of polymerization (that is, there are N_e monomers in a chain between adjacent entanglement points, and $N_e = N/N_T$). The pipe width, L_p, should be the same as the tube width, which is on the order of the entanglement length, L_e. Since $\nu = c/N$ and $N/N_e = (L_0/L_e)^2$, it follows that:

$$\kappa_1 \cong \frac{1}{\tau_R}\left(\frac{L_0}{L_e}\right)^{\alpha+2} \tag{34}$$

Now we can calculate $\mathcal{N}_1$ for the high shear band. From eq 26,

$$\mathcal{N}_1(\kappa_1) \cong \frac{ck_BT}{N_e}(\kappa_1\tau_R)^2\left(\frac{L_e}{L_0}\right)^{\beta+2} \tag{35}$$

$$\mathcal{N}_1(\kappa_1) \cong \frac{ck_BT}{N_e}\left(\frac{L_0}{L_e}\right)^{2\alpha-\beta+2} \tag{36}$$

We know that $\mathcal{N}_1(\kappa_1)$ is much larger than ck_BT/N_e, because the experimental data show that $\mathcal{N}_1$ increases steeply through the shear-banded regime. Also, this system clearly shows entangled behavior, in agreement with the reptation-breaking theory, at low and moderate shear rates, so it must have $L_0/L_p \gg 1$. It follows that:

$$2\alpha - \beta + 2 > 0 \tag{37}$$

This is an interesting result. Although satisfied by both the CMM model and the dumbbell with a true pipe constraint, the Rouse chain in a pipe has $\alpha = 2$ and $\beta = 6$ and therefore is *not* compatible with this inequality. Were such a model to apply, one would expect the normal stress difference to be a constant (or nearly so) in the shear-banded region, in stark contrast to the experimental observation for micelles. In itself, this does not rule out the Rouse chain in a pipe model for polymers, because the comparison is based on the speculation that micelles and unbreakable polymers are equivalent at high flow rates. On the other hand, the very recent data of Bercea et al.[9] on conventional polymers show some evidence of a banding effect, but with a normal stress that is increasing and very large at the highest shear rates measured.

Thus the Rouse chain in a pipe, though it alleviates some of the obvious oversimplifications of the dumbbell models, does not explain the high shear data so far available. In contrast, the two dumbbell models both give the correct qualitative features for the normal stress; however, that of CMM yields values of the parameters that agree better with estimates from other sources. In particular, the value of N_T fit by the model of a dumbbell with a true pipe constraint is much larger than that inferred from the linear viscoelastic spectrum using the method of Granek.[12]

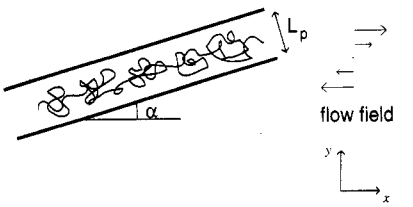

Figure 7. Modified pipe model, with the pipe oriented at angle α to the flow direction.

Various "improvements" of the Rouse chain in a pipe model can be proposed in an attempt to improve agreement with the data. For example, it could be argued that the physical tube is not perfectly aligned with the flow and instead should be modeled as a straight pipe oriented at some angle α to the streamlines, which is in general some unknown function of κ (Figure 7). The velocity gradient tensor required is now of the form:

$$\mathbf{K}^{\text{eff}} = \mathbf{K} + \mathbf{R}\cdot\mathbf{L}\cdot\mathbf{R}^{-1} \tag{38}$$

where $\mathbf{R}$ is a rotation matrix through angle α about the z-axis (by comparison with eq 18). Repeating the analysis of Appendix C with this form of $\mathbf{K}$, we either reproduce the result derived already (eqs 25 and 26) or else get a pathological answer: the stress diverges at finite shear rate. Which of these two outcomes occurs depends on the precise behavior of α as a function of κ. If the angle does not tend to zero fast enough at high flows, the chains undergo a coil–stretch transition[16] because the shear flow has an increasing elongational component along the axis of the pipe. Models based on inclined pipes do not therefore appear to offer any worthwhile improvement.

It might be possible to improve the confined Rouse model by somehow eliminating the wobble mode within each blob which seems to be responsible for the very weak stretching effect (see the discussion at the end of the last section). This could be physically motivated if one argues that the chain is entangled enough with those on neighboring streamlines to prevent the rapid transport of monomers from the upper to the lower half of the pipe (a similar excuse was made earlier for the original CMM predictions for the dumbbell). However, we have not yet succeeded in formulating a suitable variant of the Rouse model in quantitative terms.

5. Conclusions

We have in this paper discussed two dumbbell models and a confined Rouse model that attempt to describe the flow of entangled polymers at very high shear rates. The fact that all yield different results for the exponents α and β (characterizing shear and normal stresses respectively) is a surprise and also an indication that simplifications considered harmless in other contexts are dangerous here.

Of the models considered, the results given by CMM (which we have shown correspond in fact to a dumbbell with fixed transverse dimension across the flow) seem to agree best with the quantitative experimental data for micelles.[15] The model of a dumbbell with a true pipe constraint (for which the predictions differ from those of CMM) gives less agreeable fit parameters for micelles but

does at least predict a large, increasing normal stress in the shear-banded region. Disappointingly, even this qualitative feature is not reproduced by the confined Rouse model.

The experimental observation of large, increasing normal stresses provides a useful constraint (eq 37) for the exponents α and β defined by eqs 28 and 29, provided that shear banding is present. The constraint is obeyed by both dumbbell models but not the confined Rouse model, which at first sight should be much more realistic than either of the dumbbell treatments. However, the comparison with experiment depends on an untested assumption, that micelle chain breaking does not play a major role at high shear rates. The preliminary data of Bercea et al. on conventional polymers[9] shares the qualitative behavior of the normal stress, but it is not yet clear that the shear-banding picture applies to this data. The development of a more suitable model for both entangled polymers and micelles at high shear rates therefore remains a matter of urgent theoretical interest.

Acknowledgment. We are grateful to Tom McLeish for illuminating discussions. N.A.S. thanks the Science and Engineering Research Council (U.K.) and Shell Research Limited, Thornton Research Center, for receipt of a CASE award.

Appendix A

We will now rigorously analyze the dumbbell and pipe model, with a true pipe constraint (Figure 1). The bead coordinates, $\mathbf{R}_1$ and $\mathbf{R}_2$, obey the Langevin equations (8) and (9), subject to the constraint that:

$$0 \le y_1 \le L_p \tag{39}$$

$$0 \le y_2 \le L_p \tag{40}$$

Let $\Delta\mathbf{R} = \mathbf{R}_2 - \mathbf{R}_1$. Then $\Delta\mathbf{R}$ follows eq 10, of which the x-component is

$$\zeta\Delta\dot{x} + \zeta(\Delta x/\tau) = f_x + \zeta\kappa\Delta y\hat{\mathbf{x}} \tag{41}$$

Here $f_x(t)$ satisfies $\langle f_x(t)\, f_x(t')\rangle = 4\zeta k_B T\delta(t-t')$; this result arises because $f_x = f_{2x} - f_{1x}$ and $\langle f_{1x}(t)\, f_{1x}(t')\rangle = \langle f_{2x}(t)\, f_{2x}(t')\rangle = 2\zeta k_B T\delta(t-t')$.

The pipe affects only the y-motion, so Δx has no contraints. Therefore, we can simply integrate eq 41, to give

$$\Delta x(t) = \int_{-\infty}^{t}\left(\frac{1}{\zeta}f_x(t') + \kappa\Delta y(t')\right)e^{-(t-t')/\tau}\,dt' \tag{42}$$

Multiplying by Δy and performing a thermal average gives

$$\langle\Delta x(t)\,\Delta y(t)\rangle = \kappa\int_{-\infty}^{t}\langle\Delta y(t)\,\Delta y(t')\rangle e^{-(t-t')/\tau}\,dt' \tag{43}$$

and, because the problem is stationary in time, this gives

$$\langle\Delta x\Delta y\rangle = \kappa\int_0^\infty\langle\Delta y(0)\,\Delta y(t)\rangle e^{-t/\tau}\,dt \tag{44}$$

We can obtain $\langle\Delta x\Delta x\rangle$ similarly:

$$\langle\Delta x\Delta x\rangle = \frac{L_0^2}{3} + \kappa^2\int_0^\infty dt'\int_0^\infty dt''\langle\Delta y(t')\,\Delta y(t'')\rangle e^{-(t'+t'')/\tau} \tag{45}$$

and by changing the variables of integration, we find

$$\langle\Delta x\Delta x\rangle = \frac{L_0^2}{3} + \kappa^2\tau\int_0^\infty\langle\Delta y(0)\,\Delta y(t)\rangle e^{-t/\tau}\,dt \tag{46}$$

Now we must find $\langle\Delta y(0)\,\Delta y(t)\rangle$. The y-motion is independent of the shear rate, because the flow is in the x-direction, and the spring has a linear force law. Therefore, y_1 and y_2 are equivalent to the coordinates of a particle, undergoing Brownian motion in a two-dimensional space, confined to a square box of side L_p, and in the presence of a potential $(3k_BT/2L_0^2)(y_1 - y_2)^2$. Let $G(y_1,y_2,y_1',y_2',t)$ be Green's function for this process. Then:

$$\langle\Delta y(0)\,\Delta y(t)\rangle = \frac{\int_0^{L_p}dy_1\int_0^{L_p}dy_2\int_0^{L_p}dy_1'\int_0^{L_p}dy_2'(y_1-y_2)(y_1'-y_2')G(y_1,y_2,y_1',y_2',t)}{\int_0^{L_p}dy_1\int_0^{L_p}dy_2\int_0^{L_p}dy_1'\int_0^{L_p}dy_2'G(y_1,y_2,y_1',y_2',t)} \tag{47}$$

We can find G in the limit $L_p/L_0 \ll 1$, because then the potential becomes negligible. The y_1- and y_2-motions are now independent, and G factorizes

$$G(y_1,y_2,y_1',y_2',t) = g(y_1,y_1',t)\,g(y_2,y_2',t) \tag{48}$$

where g is Green's function of the one-dimensional diffusion equation with reflecting boundary conditions at 0 and L_p (and diffusion coefficient $k_BT/\zeta = L_0^2/6\tau$). Now, g is given by a series:

$$g(y,y',t) = \frac{2}{L_p}\sum_{p=1}^{\infty}\sin\left(\frac{p\pi y}{L_p}\right)\sin\left(\frac{p\pi y'}{L_p}\right)\exp\left(\frac{-p^2\pi^2 t}{6\tau}\frac{L_0^2}{L_p^2}\right) \tag{49}$$

but with $L_p/L_0 \ll 1$, we can discard all but the first term. It follows that:

$$\langle\Delta y(0)\,\Delta y(t)\rangle = \frac{L_p^2}{8}\exp\left(-\frac{\pi^2 L_0^2 t}{2L_p^2\tau}\right) \tag{50}$$

in the limit of interest; using eq 3, this gives

$$\sigma_{xy} \cong \nu k_B T\,\kappa\tau(L_p/L_0)^4 \tag{51}$$

$$\mathcal{N}_1 = n_1\nu k_B T + n_2\nu k_B T(\kappa\tau)^2(L_p/L_0)^4 \tag{52}$$

where n_1 and n_2 are numerical constants.

Appendix B

We deduce here an exact result concerning the Rouse chain in a hard-walled pipe. The Rouse chain, subject to a steady velocity gradient tensor $\mathbf{K}$, obeys the following equation:

$$\zeta\frac{\partial\mathbf{R}_n}{\partial t} - k\frac{\partial^2\mathbf{R}_n}{\partial n^2} - \zeta\mathbf{K}\cdot\mathbf{R}_n = \mathbf{f}_n \tag{53}$$

where $\mathbf{R}_n$ is the position of the nth bead, $\mathbf{f}_n$ is the Brownian force on it, ζ is the bead friction coefficient, and $k = 3k_BT/b^2$ where b is the equilibrium root-mean-square length of a spring. Transformed into normal modes, this equation becomes[1]

$$\zeta\frac{\partial\mathbf{X}_p}{\partial t} + k_p\mathbf{X}_p = \mathbf{f}_p + \zeta_p\mathbf{K}\cdot\mathbf{X}_p \tag{54}$$

where

$$\zeta_0 = N\zeta \tag{55}$$

$$\zeta_p = 2N\zeta \qquad \text{for } p = 1, 2, \ldots \tag{56}$$

$$k_p = 2\pi^2 k p^2/N \tag{57}$$

and the $\mathbf{f}_p$ are Brownian forces satisfying:

$$\langle \mathbf{f}_p \rangle = 0 \tag{58}$$

$$\langle \mathbf{f}_p(t)\, \mathbf{f}_q(t') \rangle = 2\delta_{pq}\zeta_p k_B T \delta(t-t')\, \mathbf{I} \tag{59}$$

In a steady simple shear flow, κ, this reduces to:

$$\zeta_p \frac{\partial \mathbf{X}_p}{\partial t} + k_p \mathbf{X}_p = \mathbf{f}_p + \zeta_p \kappa X_{py} \hat{\mathbf{x}} \tag{60}$$

This has the same form as eq 10 for $\Delta\mathbf{R}$ in the dumbbell problem. Of course, the constraint due to the pipe is different here; it is a set of inequalities in the X_{py}. However, the X_{px} are unconstrained, and therefore the x-coordinate of eq 60 can be integrated in precisely the same way as for the dumbbell, giving, for $p \geq 1$:

$$\langle X_{px} X_{py} \rangle = \kappa \int_0^\infty \langle X_{py}(0)\, X_{py}(t) \rangle e^{-t/\tau_p}\, dt \tag{61}$$

$$\langle X_{px} X_{px} \rangle = \frac{Nb^2}{6\pi^2}\frac{1}{p^2} + \kappa^2 \int_0^\infty dt' \int_0^\infty dt''\, \langle X_{py}(t')\, X_{py}(t'') \rangle e^{-(t'+t'')/\tau_p} \tag{62}$$

where:

$$\tau_p = \zeta_p/k_p = \tau_R/p^2 \tag{63}$$

and τ_R is the Rouse time. The y-motion is independent of the shear rate, so the integrals do not depend on κ. Since the total stress is given by summing, we have[1]

$$\sigma = \frac{c}{N}\sum_{p=1}^{\infty} k_p \langle \mathbf{X}_p \mathbf{X}_p \rangle \tag{64}$$

where c and N are the monomer concentration and the degree of polymerization, respectively. It follows that:

$$\sigma_{xy} \propto \kappa \tag{65}$$

$$\mathcal{N}_1 = C_1 + C_2\kappa^2 \tag{66}$$

where C_1 and C_2 do not depend on κ.

Appendix C

We solve here the problem of the Rouse chain, subject to shear flow, in a quadratic confining potential. The Langevin equation is eq 24:

$$\zeta \frac{\partial \mathbf{R}_n}{\partial t} - k \frac{\partial^2 \mathbf{R}_n}{\partial n^2} - \zeta \mathbf{K}^{\text{eff}} \cdot \mathbf{R}_n = \mathbf{f}_n \tag{67}$$

where the effective velocity gradient tensor is the sum of the true velocity gradient and a contribution due to the potential:

$$\mathbf{K}^{\text{eff}} = \mathbf{K} + \mathbf{L} \tag{68}$$

where

$$\mathbf{K} = \begin{pmatrix} 0 & \kappa & 0 \\ 0 & 0 & 0 \\ 0 & 0 & 0 \end{pmatrix} \tag{69}$$

$$\mathbf{L} = \begin{pmatrix} 0 & 0 & 0 \\ 0 & -\lambda & 0 \\ 0 & 0 & -\lambda \end{pmatrix} \tag{70}$$

In terms of normal modes, this becomes eq 54, with $\mathbf{K}^{\text{eff}}$ replacing $\mathbf{K}$. In the steady state, we have[1]

$$0 = \frac{2k_B T}{\zeta_p}\delta_{\alpha\beta} - \frac{2k_p}{\zeta_p}\langle X_{p\alpha} X_{p\beta} \rangle + K^{\text{eff}}_{\alpha\mu}\langle X_{p\mu} X_{p\beta} \rangle + K^{\text{eff}}_{\beta\mu}\langle X_{p\mu} X_{p\alpha} \rangle \tag{71}$$

which gives, for $p \geq 1$:

$$\frac{\langle X_{px} X_{py} \rangle}{k_B T} = \frac{\kappa\tau_p}{(1+\lambda\tau_p)(2+\lambda\tau_p)} \tag{72}$$

$$\frac{\langle X_{px} X_{px} \rangle}{k_B T} = 1 + \frac{(\kappa\tau_p)^2}{(1+\lambda\tau_p)(2+\lambda\tau_p)} \tag{73}$$

$$\frac{\langle X_{py} X_{py} \rangle}{k_B T} = \frac{1}{1+\lambda\tau_p} \tag{74}$$

τ_p is defined in eq 63. The stress tensor is

$$\sigma = \frac{c}{N}\sum_{p=1}^{\infty} k_p \langle \mathbf{X}_p \mathbf{X}_p \rangle \tag{75}$$

so

$$\sigma_{xy} = \frac{c}{N}\sum k_p \langle X_{px} X_{py} \rangle \tag{76}$$

$$\mathcal{N}_1 = \frac{c}{N}\sum k_p (\langle X_{px} X_{px} \rangle - \langle X_{py} X_{py} \rangle) \tag{77}$$

For an entangled system, the tube width is much less than the chain's radius of gyration, so $L_p \ll L_0$ and $\lambda \gg 1$. The sums can be done in this limit by replacing them with integrals, using the substitution $x = p(2/\lambda\tau_R)^{1/2}$:

$$\sigma_{xy} = \lim_{\lambda\to\infty} \frac{c}{N} k_B T \frac{\kappa}{\lambda} \sum_{p=1}^{\infty} \frac{2p^2}{\lambda\tau_R} \frac{1}{(2+2p^2/\lambda\tau_R)(1+2p^2/\lambda\tau_R)} \tag{78}$$

$$= \frac{c}{N} k_B T \frac{\kappa\tau_R}{(2\lambda\tau_R)^{1/2}} \int_0^\infty \frac{x^2\, dx}{(2+x^2)(1+x^2)} \tag{79}$$

$$\mathcal{N}_1 = \lim_{\lambda\to\infty} \frac{c}{N} k_B T \sum_{p=1}^{\infty} \left\{ \frac{2}{2+2p^2/\lambda\tau_R} + \left(\frac{\kappa}{\lambda}\right)^2 \frac{2p^2}{\lambda\tau_R} \left(\frac{1}{2p^2/\lambda\tau_R} - \frac{2}{1+2p^2/\lambda\tau_R} + \frac{1}{2+2p^2/\lambda\tau_R} \right) \right\} \tag{80}$$

$$\mathcal{N}_1 = \frac{c}{N}k_B T\left(\frac{\lambda\tau_R}{2}\right)^{1/2}\int_0^\infty dx\left\{\frac{2}{x^2+2} + 2\left(\frac{\kappa}{\lambda}\right)^2\frac{1}{(1+x^2)(2+x^2)}\right\} \quad (81)$$

Finally, we must estimate λ. The end-to-end vector of the chain is[1]

$$\mathbf{P} = -4\sum_{p=\text{odd}}\mathbf{X}_p \quad (82)$$

so the mean-square y-component is

$$\langle P_y^2\rangle = 16k_B T\sum_{p=\text{odd}}\frac{1}{k_p + \lambda\zeta_p} \quad (83)$$

$$\langle P_y^2\rangle = \frac{16k_B T}{\lambda\zeta_1}\sum_{p=\text{odd}}\frac{1}{1 + p^2/\lambda\tau_R} \quad (84)$$

Again taking the limit $\lambda \to \infty$, and with $x = p/(\lambda\tau_R)^{1/2}$, we obtain

$$\langle P_y^2\rangle = \frac{8k_B T}{\lambda\zeta_1}(\lambda\tau_R)^{1/2}\int_0^\infty\frac{dx}{1+x^2} \quad (85)$$

Now, $\zeta_1/k_1 = \tau_R = Nb^2\zeta_1/6\pi^2 k_B T$, so $k_B T/\zeta_1 \cong Nb^2/\tau_R = L_0^2/\tau_R$. Therefore:

$$\langle P_y^2\rangle \cong L_0^2/(\lambda\tau_R)^{1/2} \quad (86)$$

$\langle P_y^2\rangle$ must be of order L_p^2, so

$$\lambda \cong \frac{1}{\tau_R}\left(\frac{L_0}{L_p}\right)^4 \quad (87)$$

It follows that:

$$\sigma_{xy} \cong (c/N)k_B T\kappa\tau_R(L_p/L_0)^2 \quad (88)$$

$$\mathcal{N}_1 = n_4(c/N)k_B T(L_p/L_0)^{-2} + n_5(c/N)k_B T(\kappa\tau_R)^2(L_p/L_0)^6 \quad (89)$$

where n_4 and n_5 are numerical constants.

References and Notes

(1) Doi, M.; Edwards, S. F. *The Theory of Polymer Dynamics*; Clarendon Press: Oxford, U.K., 1986.
(2) McLeish, T. C. B. Ph.D. Thesis, University of Cambridge, Cambridge, U.K., 1987. McLeish, T. C. B.; Ball, R. C. *J. Polym. Sci., Part B: Polym. Phys.* **1986**, *24*, 1735.
(3) Marrucci, G.; Grizzuti, N. *Gazz. Chim. Ital.* **1988**, *118*, 179.
(4) Pearson, D.; Herbolzheimer, E.; Grizzuti, N.; Marrucci, G. *J. Polym. Sci., Part B: Polym. Phys.* **1991**, *29*, 1589.
(5) Cates, M. E.; McLeish, T. C. B.; Marrucci, G. *Europhys. Lett.* **1993**, *21*, 451.
(6) Larson, R. G. *Constitutive Equations for Polymer Melts and Solutions*; Butterworth: Stoneham, MA, 1988.
(7) de Gennes, P.-G. *Scaling Concepts in Polymer Physics*; Cornell University Press: Ithaca, NY, 1979.
(8) Yerushalmi, J.; Katz, S.; Shinnar, R. *Chem. Eng. Sci.* **1970**, *25*, 1891.
(9) Bercea, M.; Peiti, C.; Simionescu, B.; Navard, P., to appear in *Macromolecules*.
(10) Cates, M. E.; Candau, S. J. *J. Phys.: Condens. Matter* **1990**, *2*, 6869.
(11) Cates, M. E. *Macromolecules* **1987**, *20*, 2289. Cates, M. E. *J. Phys. Chem.* **1990**, *94*, 371.
(12) Granek, R.; Cates, M. E. *J. Chem. Phys.* **1992**, *96*, 4758.
(13) Turner, M. S.; Cates, M. E. *Langmuir* **1991**, *7*, 1590.
(14) Rehage, H.; Hoffmann, H. *Mol. Phys.* **1991**, *74*, 933.
(15) Spenley, N. A.; Cates, M. E.; McLeish, T. C. B. *Phys. Rev. Lett.* **1993**, *71*, 939.
(16) de Gennes, P.-G. *J. Chem. Phys.* **1974**, *60*, 5030.